

Chapter 5

High-energy phenomenology

5.1 Deep inelastic scattering

From elastic eN scattering one can extract the nucleon's electromagnetic form factors. In a general *inelastic* scattering process the nucleon does not stay intact; instead it breaks up and produces hadronic final states. Depending on the invariant mass of the hadronic end product, the inelastic cross section then contains nucleon resonance peaks and nucleon-meson continua. Moreover, **deep inelastic scattering (DIS)** has given us first convincing evidence for the existence of quarks since it probes the composite nature of the nucleon. In DIS the transferred momentum of the photon is so large that it strikes the perturbative ‘partons’ inside the nucleon, which allows us to describe the longitudinal momentum distributions of the quarks and gluons through parton distribution functions.

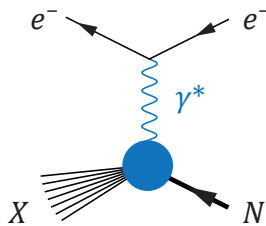


FIG. 5.1: DIS

Phase space. Employing the variables (4.5.8–4.5.9) with massless electrons ($m = m' = 0$), there are three independent Lorentz invariants: the spacelike momentum transfer $\tau = Q^2/(4M^2) \geq 0$, the crossing variable λ , and the invariant mass $W = M'$ of the hadrons in the final state which is no longer fixed but also a variable. The kinematic phase space of the process, which in elastic scattering was described by the two-dimensional Mandelstam plane, thus becomes three-dimensional. Instead of W , we could work with either of the variables ω , ν or the Bjorken variable x defined in Eq. (4.5.16):

$$W = M\sqrt{1 + 4\omega}, \quad \omega + \tau = \frac{\nu}{2M} = \frac{\tau}{x}. \quad (5.1.1)$$

Below we will see that in the one-photon exchange approximation the cross section factorizes again into a leptonic and a hadronic part, where the hadronic subprocess only depends on τ and ω .

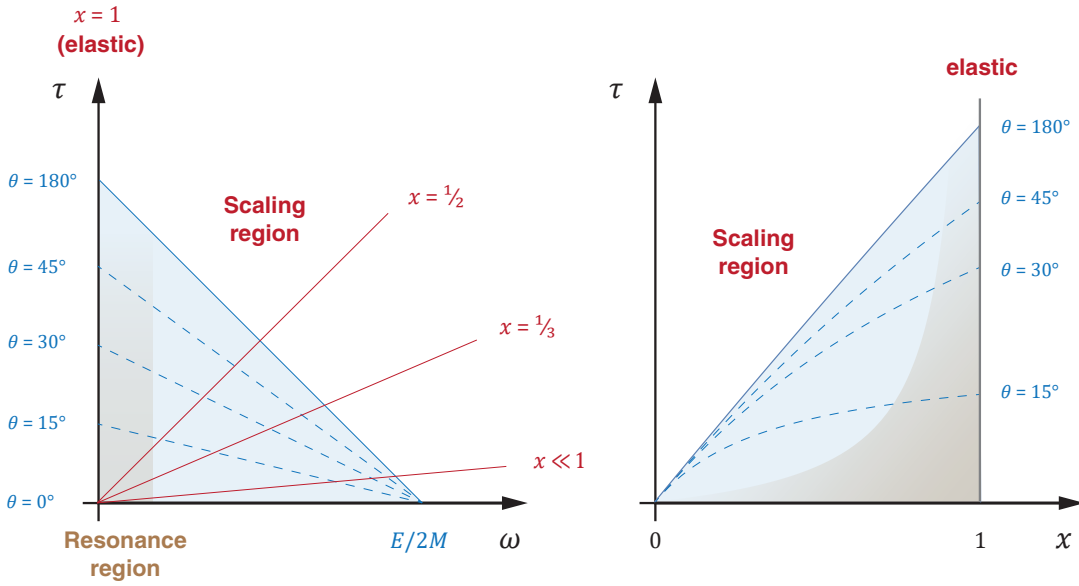


FIG. 5.2: Kinematic phase space in inelastic eN scattering at fixed lepton energy E in the variables (ω, τ) , left, and (x, τ) , right. The physical region is shown in blue and the resonance region in brown. Lines of constant scattering angle θ and Bjorken- x are also included.

To relate the Lorentz invariants to the incoming lepton energy E and the scattering angle θ in the lab frame, we infer from the relations (4.5.38):

$$\tau = (\varepsilon - \omega) \frac{4\varepsilon \sin^2 \frac{\theta}{2}}{1 + 4\varepsilon \sin^2 \frac{\theta}{2}} = \varepsilon x \frac{4\varepsilon \sin^2 \frac{\theta}{2}}{x + 4\varepsilon \sin^2 \frac{\theta}{2}}, \quad \varepsilon := \frac{E}{2M}. \quad (5.1.2)$$

The resulting phase space in the (ω, τ) and (x, τ) planes is sketched in Fig. 5.2. For fixed lepton energy E , the physically allowed region is bounded by $\omega = 0 \Leftrightarrow x = 1$ (elastic scattering), $\tau = 0$ (forward angles $\theta = 0$), and backward angles $\theta = \pi$ which for large energies implies $\tau \approx \varepsilon - \omega \approx \varepsilon x$. This is the blue area in the plot, whose size is characterized by the external control parameter E : if we increase the energy of the lepton beam, we can reach higher τ and ω values. We can locate different regions in these plots:

- At the elastic threshold $\omega = 0 \Leftrightarrow x = 1$, the invariant mass is $W = M$. The region $W \gtrsim M$ (or $\omega \lesssim 1$) is the **resonance region** where nucleon resonances appear in the cross section, starting with the $\Delta(1232)$ peak as shown in Fig. 5.3. Above $W \sim 2$ GeV, there is no visible resonance structure left.
- The limit $\tau + \omega \rightarrow \infty$ and $\omega/\tau = \text{const.}$ defines the **Bjorken limit**: this is the DIS region where scaling occurs. From Eq. (5.1.1) the Bjorken limit corresponds to $\nu \rightarrow \infty$ and constant Bjorken- x .
- The region of small x is interesting for several reasons and assumed to give experimental access to the properties of gluons.

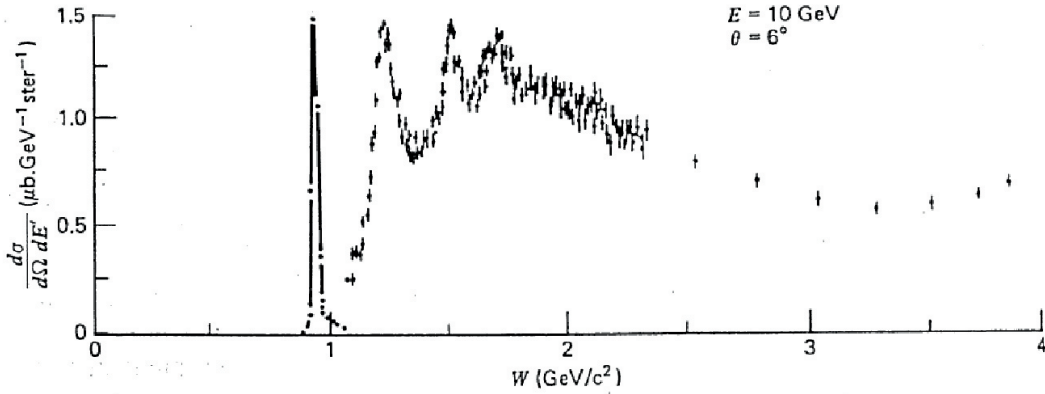


FIG. 5.3: Double-differential inelastic eN cross section from Eq. (5.1.11) at fixed lepton energy E and scattering angle θ . At large invariant masses, the resonance peaks are washed out. (*Halzen and Martin, Quarks and Leptons: An Introductory Course in Modern Particle Physics, Wiley, 1984.*)

Cross section and structure functions. Let us work out the cross section for inelastic eN scattering. In an inclusive measurement only the outgoing electron is detected but not the remnants of the proton. The cross section in the one-photon approximation still has the generic form of Eqs. (4.5.41–4.5.42) with the same leptonic tensor (4.5.67). However, the hadronic contribution to the invariant matrix element $|\mathcal{M}|^2$ and to the phase space factor now sums over all possible final states,

$$d\sigma = \frac{1}{4ME} \frac{d^3k_f}{(2\pi)^3 2E'} \frac{e^4}{q^4} L_{\mu\nu} 4\pi M W^{\mu\nu},$$

$$4\pi M W^{\mu\nu} = \sum_X \frac{d^3p_f}{(2\pi)^3 2E_X} \langle N(p_i) | V_{\text{em}}^\mu(0) | X(p_f) \rangle \langle X(p_f) | V_{\text{em}}^\nu(0) | N(p_i) \rangle \quad (5.1.3)$$

$$\times (2\pi)^4 \delta^4(q + p_i - p_f).$$

Here we absorbed the integral over d^3p_f and the δ -function for energy-momentum conservation into a hadronic tensor $W^{\mu\nu}$, and V_{em}^μ is the electromagnetic current operator from Eq. (3.1.92) that enters in the electromagnetic transition from the nucleon to all possible final states X .

Observe that the hadronic tensor comprises the completeness relation (2.2.5). If we write the δ -function in momentum space as

$$(2\pi)^4 \delta^4(q + p_i - p_f) = \int d^4z e^{i(q+p_i-p_f)z}, \quad (5.1.4)$$

use translation invariance (2.2.10–2.2.11) to shuffle the z -dependence in the phase factor $e^{i(p_i-p_f)z}$ into the current operators, and sum over the complete set of states X , we obtain:

$$4\pi M W^{\mu\nu}(p, q) = \int d^4z e^{iqz} \langle N(p_i) | V_{\text{em}}^\mu\left(\frac{z}{2}\right) V_{\text{em}}^\nu\left(-\frac{z}{2}\right) | N(p_i) \rangle$$

$$= \int d^4z e^{iqz} \langle N(p_i) | [V_{\text{em}}^\mu\left(\frac{z}{2}\right), V_{\text{em}}^\nu\left(-\frac{z}{2}\right)] | N(p_i) \rangle. \quad (5.1.5)$$

In the second line we replaced the product of the currents by their commutator because the matrix element of $V_{\text{em}}^\nu(-\frac{z}{2})V_{\text{em}}^\mu(\frac{z}{2})$ is zero: it gives rise to a δ -function $\delta(q-p_i+p_f)$ which cannot be saturated by any intermediate state. Energy conservation would require $E_X = M - E + E' = M - \nu \leq M$, but the nucleon is the lightest ground-state baryon. In this way, the hadronic tensor is the matrix element of the current commutator, which is analogous to the commutators in Eq. (3.1.58) and vanishes outside the light cone. We will return to this expression later.

For now, let us work out the general form of the hadronic tensor $W^{\mu\nu}(p, q)$ in momentum space. For unpolarized scattering, it can only depend on the Lorentz tensors

$$T_q^{\mu\nu}, \quad p_T^\mu p_T^\nu, \quad q^\mu q^\nu, \quad p_T^\mu q^\nu \pm q^\mu p_T^\nu, \quad (5.1.6)$$

where $T_q^{\mu\nu} = g^{\mu\nu} - q^\mu q^\nu / q^2$ is the transverse projector and $p_T^\mu = T_q^{\mu\nu} p_\nu$ the momentum transverse to q^μ . Current conservation still holds because the sum of the outgoing charges must equal the nucleon charge, so $W^{\mu\nu}$ must be transverse in its Lorentz indices: $q_\mu W^{\mu\nu} = W^{\mu\nu} q_\nu = 0$. The most general transverse tensor according to these constraints is given by

$$W^{\mu\nu} = -W_1(\tau, \omega) T_q^{\mu\nu} + \frac{W_2(\tau, \omega)}{M^2} p_T^\mu p_T^\nu, \quad (5.1.7)$$

where the response functions W_1 and W_2 depend on the Lorentz invariants τ and ω . From these one defines the dimensionless **nucleon structure functions** as

$$F_1(\tau, \omega) = M W_1(\tau, \omega), \quad F_2(\tau, \omega) = \nu W_2(\tau, \omega). \quad (5.1.8)$$

(For polarized scattering, there are two further spin-dependent structure functions g_1, g_2 and there is also another term in the lepton tensor.)

Combining this with the leptonic tensor yields

$$\begin{aligned} L^{\mu\nu} W_{\mu\nu} &= 4 \left[\frac{W_2}{M^2} \left((p \cdot k)^2 + \frac{q^2}{4} p_T^2 \right) - W_1 \left(k^2 + \frac{3}{4} q^2 \right) \right] \\ &= 4M^2 [W_2 (\lambda^2 - (\tau + \omega)^2 - \tau) + 2W_1 \tau] \\ &= 4EE' \cos^2 \frac{\theta}{2} \left[W_2 + 2W_1 \tan^2 \frac{\theta}{2} \right]. \end{aligned} \quad (5.1.9)$$

In going from the first to the second line we used $k_T^\mu = k^\mu$, $p \cdot k = M^2 \lambda$, $k^2 = M^2 \tau$ and

$$p_T^2 = p^2 - \frac{(p \cdot q)^2}{q^2} = M^2 \left(1 + 2\omega + \tau + \frac{\omega^2}{\tau} \right) = \frac{M^2}{\tau} (\tau + (\tau + \omega)^2), \quad (5.1.10)$$

and to obtain the third line we exploited Eqs. (4.5.36) and (4.5.38). The resulting cross section, which is shown in Fig. 5.3, is

$$\frac{d^2\sigma}{d\Omega dE'} = \frac{\alpha^2}{q^4} \frac{E'}{E} L_{\mu\nu} W^{\mu\nu} = \frac{\alpha^2 \cos^2 \frac{\theta}{2}}{4E^2 \sin^4 \frac{\theta}{2}} \left[W_2 + 2W_1 \tan^2 \frac{\theta}{2} \right]. \quad (5.1.11)$$

How does this compare to the limit of elastic scattering? From (4.5.44) and (4.5.71) we can write down the double-differential cross section for a pointlike fermion in the elastic case:

$$\begin{aligned} \frac{d^2\sigma}{d\Omega dE'} &= \frac{|\mathcal{M}|^2}{4ME} \frac{1}{(4\pi)^2} \frac{E' \delta(\omega)}{2M^2} = \frac{\alpha^2}{4M^2\tau^2} \frac{E'}{E} \frac{\delta(\omega)}{2M} (\lambda^2 + \tau^2 - \tau) \\ &= \frac{\alpha^2 \cos^2 \frac{\theta}{2}}{4E^2 \sin^4 \frac{\theta}{2}} \frac{\delta(\omega)}{2M} \left(1 + 2\tau \tan^2 \frac{\theta}{2}\right). \end{aligned} \quad (5.1.12)$$

Hence, in the elastic limit the response functions reduce to

$$W_1(\tau, \omega) = \tau \frac{\delta(\omega)}{2M}, \quad W_2(\tau, \omega) = \frac{\delta(\omega)}{2M}. \quad (5.1.13)$$

We can trade the dependence on ω by a dependence on the Bjorken variable x using the relations

$$\tau = \frac{\nu}{2M} x, \quad \omega = \frac{\nu}{2M} (1 - x). \quad (5.1.14)$$

As a consequence, when expressed in terms of τ and x , the structure functions defined in Eq. (5.1.14) become

$$\begin{aligned} F_1(\tau, x) &= M W_1(\tau, x) = \frac{1}{2} \delta(1 - x), \\ F_2(\tau, x) &= \nu W_2(\tau, x) = \delta(1 - x). \end{aligned} \quad (5.1.15)$$

We see that for elastic scattering on a pointlike particle, the dimensionless structure functions $F_1(\tau, x)$ and $F_2(\tau, x)$ are functions of x only; in addition, the δ -function enforces $x = 1$ in the elastic limit.

For scattering on a composite nucleon, the expressions (5.1.13) in the elastic limit must be multiplied with the Sachs form factor combinations in the Rosenbluth cross section (4.5.77). Here one should remember not to confuse the structure functions F_1 and F_2 with the equally named Dirac and Pauli form factors. In fact, even their physical meanings are reversed: By comparing the two cross sections, one can see that W_1 encodes the spin of the target and vanishes for a spinless particle. Thus, the structure function F_1 carries the spin dependence, whereas in the form factor case it is rather the Pauli form factor (or the magnetic form factor G_M) that contains the nucleon spin.

Bjorken scaling and the parton model. One might expect that for inelastic scattering processes ($x \neq 1$), away from the nucleon resonance region, the structure functions F_1 and F_2 are complicated functions of τ and x . However, it turns out that in the DIS region they are almost independent of τ and only functions of x :

$$F_{1,2}(\tau, x) \approx F_{1,2}(x). \quad (5.1.16)$$

This is visible in the left of Fig. 5.4 and called **Bjorken scaling**. Another observation is the **Callan-Gross relation**, which implies that F_1 and F_2 are not independent:

$$F_2(x) = 2xF_1(x). \quad (5.1.17)$$

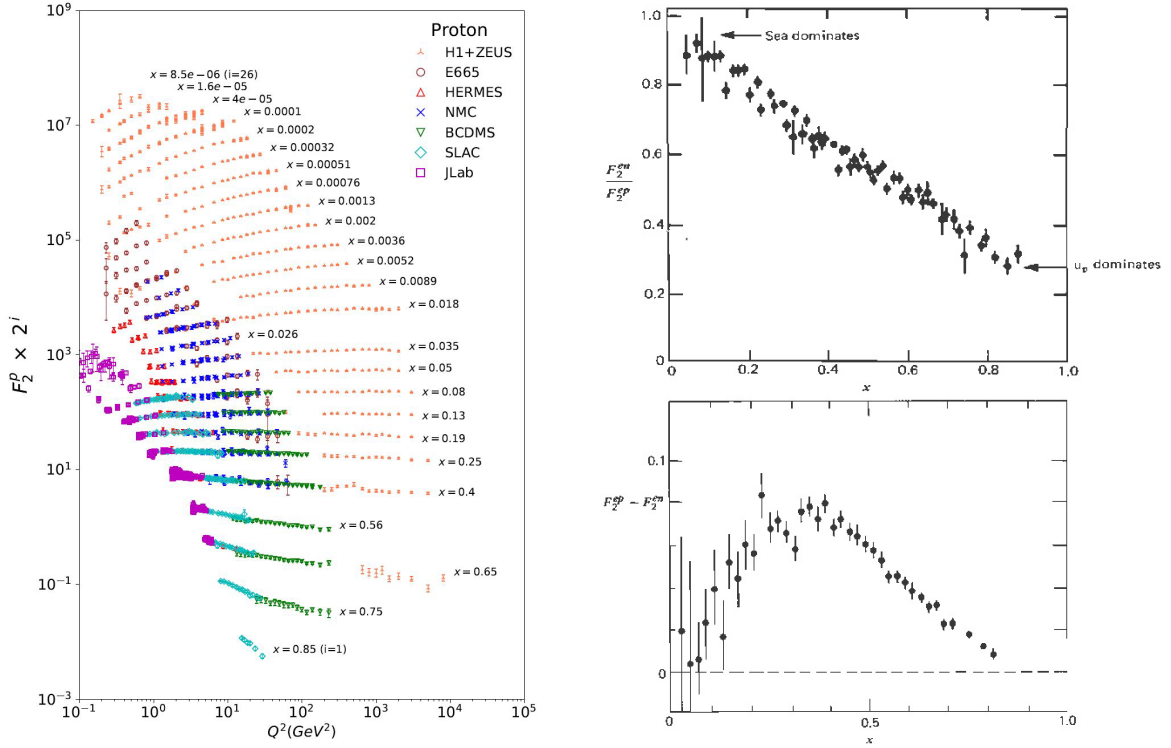


FIG. 5.4: *Left:* scaling behavior in the structure function $F_2(Q^2, x)$, PDG 2020, P. A. Zyla et al., Prog. Theor. Exp. Phys. **2020**, 083C01 (2020). *Right:* experimental data for the ratio and difference of proton and neutron structure functions in Eq. (5.1.29). Source: Halzen and Martin (see Fig. 5.3).

The origin of scaling can be understood from dimensional arguments, which follow from the near scale invariance of massless perturbative QCD (up to logarithmic corrections). A dimensionless function can only depend on dimensionless variables. τ and ω are only dimensionless because we scaled the momenta with the nucleon mass M , which requires the presence of a nonperturbative nucleon mass to begin with. If we scatter instead on (nearly) massless quarks, no such scale is available and therefore the dimensionless structure functions cannot depend on τ and ω individually but only on their dimensionless combination $\tau/\omega \sim q^2/p \cdot q$. Hence, the observation of scaling is an indication for the composite nature of the nucleon in terms of pointlike, essentially massless quarks and gluons.

The experimental observation of Bjorken scaling has led to the development of the **parton model**. Here the proton is viewed as a collection of ‘partons’, namely valence quarks, sea quarks and gluons. The incoming momentum p_i of the proton (mass M) is the sum of the parton momenta, $p_i = \sum_k p_k$, where p_k is the four-momentum of a single onshell parton with mass m_k . The basic assumption we need in the following is **collinearity**: $p_k = \xi_k p_i$, which can be justified in the **infinite momentum frame**. If we write

$$p_i = \begin{pmatrix} \sqrt{\mathbf{p}^2 + M^2} \\ \mathbf{p} \end{pmatrix}, \quad p_k = \begin{pmatrix} \sqrt{\xi_k^2 \mathbf{p}^2 + (\mathbf{p}_k^\perp)^2 + m_k^2} \\ \xi_k \mathbf{p} + \mathbf{p}_k^\perp \end{pmatrix}, \quad (5.1.18)$$

then ξ_k defines the longitudinal momentum fraction of parton k in the direction of the proton's three-momentum \mathbf{p} . In the infinite-momentum frame ($|\mathbf{p}| \rightarrow \infty$) we can neglect the transverse components and masses:

$$|\mathbf{p}_k^\perp| \ll |\mathbf{p}|, \quad m_k \ll |\mathbf{p}|, \quad \Rightarrow \quad p_k \approx \xi_k p_i, \quad \sum_k \xi_k = 1. \quad (5.1.19)$$

The collinearity assumption allows for a simple interpretation of the Bjorken scaling variable. We know from Eq. (4.5.16) that elastic scattering on the nucleon corresponds to $x = -q^2/(2p_i \cdot q) = 1$. In the inelastic process ($x \neq 1$), elastic scattering on a single parton k then entails that

$$x_k := -\frac{q^2}{2p_k \cdot q} = -\frac{q^2}{2p_i \cdot q} \frac{1}{\xi_k} = \frac{x}{\xi_k} = 1 \quad \Rightarrow \quad \xi_k = x. \quad (5.1.20)$$

In this way, the Bjorken variable x assumes the meaning of the parton's **longitudinal momentum fraction** in the infinite-momentum frame. The photon only couples to those partons whose momentum fraction is $\xi_k = x$, hence a measurement of the structure function $F_2(x)$ allows us to 'see' how the parton momenta are distributed inside the proton. In elastic scattering we have $x = 1$ and the photon couples to the whole proton since it carries the full momentum. Note that if we want to guarantee $p_i^2 = M^2$, we should set \mathbf{p}_k^\perp and $m_k = \xi_k M$. Although this last relation is a bit nonsensical as it would imply that the 'mass' of a parton changes with its momentum fraction, we need it for consistency of the naive parton model.

Let us define the **parton distribution function** or **PDF** as the momentum distribution $f_k(\xi)$ of a parton in the hadron, so that $f_k(\xi) d\xi$ is the probability density that a parton carries a momentum fraction between ξ and $\xi + d\xi$. Momentum conservation implies

$$\sum_k \int_0^1 d\xi \xi f_k(\xi) = 1. \quad (5.1.21)$$

Now suppose we scatter on spin- $\frac{1}{2}$ quarks. Using the relations (5.1.14) with $x_k = x/\xi_k$ and $m_k = \xi_k M$, the structure functions $F_j^{(k)}$ with $j = 1, 2$ for the parton k are

$$\begin{aligned} 2F_1^{(k)} &= 2MW_1^{(k)} = \frac{M}{m_k} 2m_k W_1^{(k)} = \frac{M}{m_k} x_k \delta(1 - x_k) = \delta(\xi_k - x), \\ F_2^{(k)} &= \nu W_2^{(k)} = \delta(1 - x_k) = \frac{\xi_k^2}{x} \delta(\xi_k - x) = x \delta(\xi_k - x), \end{aligned} \quad (5.1.22)$$

and integrating over all partons yields

$$F_j(x) = \sum_k e_k^2 \int d\xi f_k(\xi) F_j^{(k)}(\xi, x) \quad \Rightarrow \quad \begin{aligned} F_1(x) &= \frac{1}{2} \sum_k e_k^2 f_k(x), \\ F_2(x) &= x \sum_k e_k^2 f_k(x). \end{aligned} \quad (5.1.23)$$

Hence we have shown that in the parton model F_1 and F_2 are indeed only functions of x , and we can confirm the Callan-Gross relation (5.1.16). The latter is also an experimental indication for the spin- $\frac{1}{2}$ nature of the quarks: if quarks had spin zero, $F_1(x)$ would vanish.

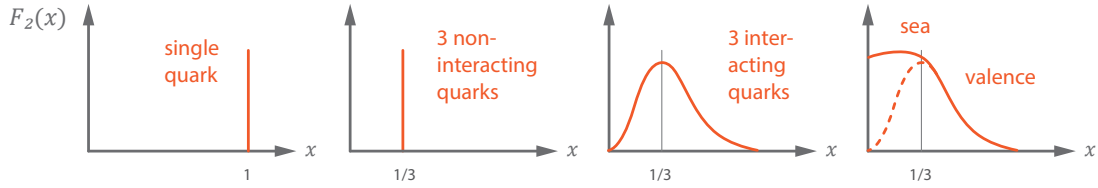


FIG. 5.5: Structure functions for different compositions of the proton.

Due to the Callan-Gross relation only the structure function $F_2(x)$ will be relevant in what follows. What does it look like? If the proton consisted of a single ‘quark’ that carried all of its momentum, the structure function would have a single peak at $x = 1$ (see Fig. 5.5). If it consisted of three non-interacting quarks, the quarks would all carry the same momentum fraction and $F_2(x)$ would have a peak at $x = \frac{1}{3}$. If the three quarks interact with each other, they can exchange momentum and hence the momentum fraction carried by each quark will fluctuate; the resulting structure function is a smooth distribution peaked near $x = \frac{1}{3}$. Finally, the presence of sea quarks will lead to an enhancement at small x because sea quarks are created in Bremsstrahlung-like processes which are typically enhanced at small momenta and lead to $xf(x) \xrightarrow{x \rightarrow 0} \text{const.}$ Note that gluons will also contribute to the momentum sum rule (5.1.21) whereas the structure function only probes electrically charged partons (quarks).

Parton distribution functions. Now let’s see how much information on the PDFs we can gather from experimental data on $F_2(x)$. There is no sensible way to distinguish two identical partons within a proton, but we can still group them according to the various quark and antiquark flavors: $f_k(x) = u(x), \bar{u}(x), d(x), \bar{d}(x)$, etc., so that we have

$$\frac{F_2^p(x)}{x} = q_u^2 ((u(x) + \bar{u}(x)) + q_d^2 (d(x) + \bar{d}(x)) + q_s^2 (s(x) + \bar{s}(x)) + \dots \quad (5.1.24)$$

It is usually sufficient to stop at the strange quark because the probability for finding charm in the proton is very small. $u(x)$ is the probability distribution for up quarks in the proton, $\bar{u}(x)$ that of anti-up quarks, and so on. One can also measure the structure function F_2^n of the neutron via electron-deuteron scattering. Charge symmetry entails that the d distribution in the neutron is identical to the u distribution in the proton: $u = u^p = d^n$, $d = d^p = u^n$, $s = s^p = s^n$, and analogously for the antiquark PDFs:

$$\frac{F_2^n(x)}{x} = q_d^2 ((u(x) + \bar{u}(x)) + q_u^2 (d(x) + \bar{d}(x)) + q_s^2 (s(x) + \bar{s}(x)) + \dots \quad (5.1.25)$$

In the following it will be more convenient to work with valence- and sea-quark distributions, defined via

$$\begin{aligned} u &= u_v + u_s, & \bar{u} &= \bar{u}_s, & s &= s_s, \\ d &= d_v + d_s, & \bar{d} &= \bar{d}_s, & \bar{s} &= \bar{s}_s, \end{aligned} \quad (5.1.26)$$

because antiquarks and strange quarks can only appear in the sea. Now, since the PDFs are number densities defined on the momentum fraction x , the integrals over

this range are just the total flavor numbers of each quark type:

$$\int_0^1 dx u_v(x) = 2, \quad \int_0^1 dx d_v(x) = 1, \quad \int_0^1 dx [f_s(x) - \bar{f}_s(x)] = 0. \quad (5.1.27)$$

The third relation expresses fermion number conservation for each flavor $f = u, d, s$: by summing over all individual partons, we must recover charge 1, baryon number 1 and strangeness 0 of the proton.

Can we extract the valence and sea distributions from the data for $F_2^{p,n}(x)$? We have two measured quantities but too many unknowns. Let's make the further simplifying assumption that all sea-quark distributions are identical: $f_s(x) = \bar{f}_s(x) =: S(x)$. Then the structure functions for the proton and neutron become

$$\begin{aligned} \frac{F_2^p(x)}{x} &= q_u^2 u_v(x) + q_d^2 d_v(x) + (q_u^2 + q_d^2 + q_s^2) 2S(x), \\ \frac{F_2^n(x)}{x} &= q_d^2 u_v(x) + q_u^2 d_v(x) + (q_u^2 + q_d^2 + q_s^2) 2S(x), \end{aligned} \quad (5.1.28)$$

from where we can form their ratio and their difference:

$$R = \frac{F_2^n}{F_2^p} = \frac{u_v + 4d_v + 12S}{4u_v + d_v + 12S}, \quad F_2^p - F_2^n = \frac{x}{3}(u_v - d_v). \quad (5.1.29)$$

The ratio satisfies the **Nachtman inequality** $\frac{1}{4} \leq R(x) \leq 4$: in a region of x where the up (down) quarks dominate, we have $R = \frac{1}{4}$ ($R = 4$); if the sea quarks dominate we will find $R = 1$. The ratio is plotted in Fig. 5.4 and reveals that the sea quarks are indeed dominant at small x whereas valence up quarks are important at large x . The difference in (5.1.29) is also plotted: it measures only the valence-quark contribution and shows a peak around $x = 1/3$, as we had expected. Finally, the sum

$$\frac{9}{5}(F_2^p + F_2^n) = x \left(u_v + d_v + \frac{24}{5} S \right) \quad (5.1.30)$$

can be plugged into the momentum sum rule (5.1.21) which now takes the form

$$\int dx x (u_v + d_v + 6S) + \varepsilon = 1, \quad (5.1.31)$$

where ε is the gluon contribution to the proton's longitudinal momentum. From the experimental data we can roughly estimate

$$\frac{9}{5} \int dx (F_2^p + F_2^n) \approx 0.54 \approx 1 - \varepsilon, \quad (5.1.32)$$

which entails that the gluons carry almost half of the proton's momentum. In fact, the gluon PDFs dominate at small values of x , see Fig. 5.6.

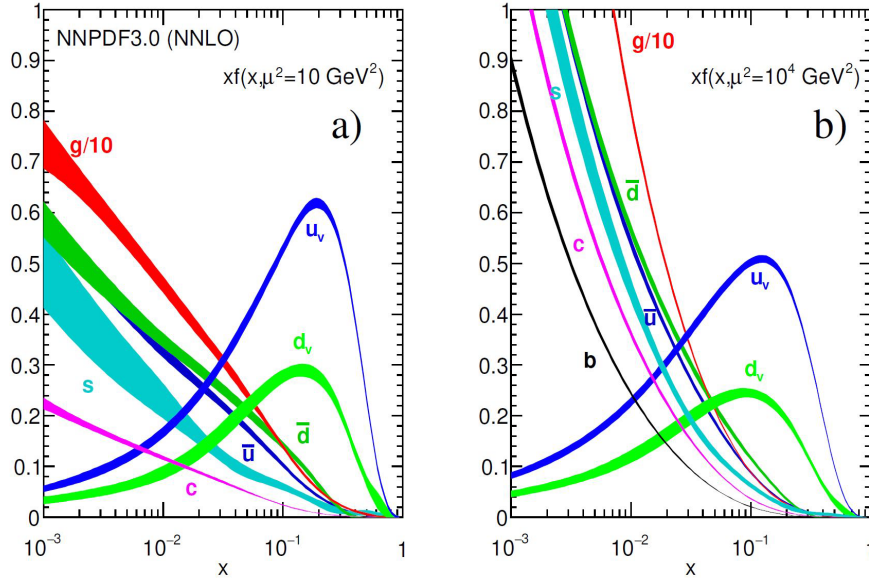


FIG. 5.6: Valence, sea-quark and gluon PDFs shown at two different resolution scales (PDG, same reference as in Fig. 5.4).

How good is the assumption that all sea-quark distributions are identical? If we go back to the original equations (5.1.24) and (5.1.25), take their difference and integrate over x , we have

$$\int dx \frac{F_2^p - F_2^n}{x} = \frac{1}{3} \int dx (u_v - d_v + u_s + \bar{u}_s - d_s - \bar{d}_s) \stackrel{(5.1.27)}{=} \frac{1}{3} + \frac{2}{3} \int dx (\bar{u}_s - \bar{d}_s)$$

which should equal $\frac{1}{3}$ if $\bar{u}_s = \bar{d}_s = S$ (this is the **Gottfried sum rule**). Instead, the experimental value is $\sim 0.23 \Rightarrow \int dx (\bar{d}_s - \bar{u}_s) \sim 0.15$, which entails that the light quark sea is indeed flavor-asymmetric.

Scaling violations. The left plot in Fig. 5.4 demonstrates that scaling is not exact because the structure functions show a Q^2 dependence, which is most pronounced at small and large values of x . In terms of the PDFs, this implies that their x -dependence is not completely independent of the resolution scale Q^2 but also evolves with Q^2 , which can be seen in Fig. 5.6. We can intuitively understand this as follows: a photon with intermediate Q^2 does not resolve the full spatial structure of the proton and mainly sees three interacting quarks, together with parts of the sea. In contrast, a high- Q^2 photon can resolve small distances and will reveal more and more of the quark sea which contains short-distance processes such as gluon emission from a quark or gluon splitting into $q\bar{q}$ pairs. As a result, the sea-quark contributions will be more prominent at higher Q^2 . On the other hand, since the photon can resolve more partons, momentum conservation implies that each parton now carries a smaller fraction of the total momentum, and hence the PDFs will be shifted to smaller x . The resulting structure function $F_2(x)$ that sums up the individual quark PDFs will rise with higher Q^2 at small x and fall with higher Q^2 at large x .

The short-distance dynamics depend on the resolution scale through the coupling $\alpha_s(Q^2)$. As a consequence, the individual quark structure functions F_i^k will no longer be mere δ -functions as in Eq. (5.1.22) but also inherit a Q^2 dependence from the coupling. Since the coupling is dimensionless, it also introduces a scale μ (the **factorization scale**), so that Eq. (5.1.23) becomes

$$F_j(x, Q^2) = \sum_k e_k^2 \int d\xi f_k(\xi, \mu) F_j^{(k)}(\xi, x, \frac{Q^2}{\mu^2}). \quad (5.1.33)$$

The $F_j^{(k)}$ encode the short-distance splitting processes and are calculable in perturbative QCD. The PDFs f_k , which now also depend on μ , are inherently nonperturbative and have to be fitted to experimental data or calculated with nonperturbative methods.

Because the nucleon structure function must be independent of the factorization scale μ , its total derivative with respect to μ must vanish. Similarly to the Callan-Symanzik equation (2.3.66), one then derives the **DGLAP equations** (Dokshitzer, Gribov, Lipatov, Altarelli, Parisi) $dF_j/d\mu = 0$. They relate PDFs at different μ with each other and thereby allow one to calculate the scaling violations using QCD perturbation theory.

Compton amplitude and PDFs. How can PDFs be calculated nonperturbatively? Let us return to the hadronic tensor $W^{\mu\nu}(q)$ from Eq. (5.1.5) which enters in the inelastic eN cross section. By means of the optical theorem, it can be written as the imaginary part of the nucleon's **forward Compton scattering amplitude**: $4\pi M W^{\mu\nu}(p, q) = 2 \text{Im} T^{\mu\nu}(p, q)$. The forward Compton amplitude $N\gamma^* \rightarrow N\gamma^*$ is given by

$$T^{\mu\nu}(p, q) = i \int d^4z e^{iqz} \langle N(p_i) | T V_{\text{em}}^\mu(\frac{z}{2}) V_{\text{em}}^\nu(-\frac{z}{2}) | N(p_i) \rangle. \quad (5.1.34)$$

If we apply the kinematics in Eqs. (4.5.8–4.5.9), then in the forward limit (vanishing momentum transfer) we have $p = p_i = p_f$ and the photon momentum is $k = k_i = k_f$, so that k^2 and the crossing variable λ are the independent Lorentz-invariants. The variables τ and x defined in DIS are related to these by

$$\tau = -\frac{k^2}{4M^2}, \quad x = -\frac{k^2}{2p \cdot k} = \frac{2\tau}{\lambda}. \quad (5.1.35)$$

Thus, the structure functions, which depend on τ and x , can be expressed through the Lorentz-invariant form factors of the Compton amplitude in the forward limit, which depend on those same variables. The Mandelstam variables s and u in Compton scattering are given by

$$\left\{ \begin{matrix} s \\ u \end{matrix} \right\} = (p \pm k)^2 = M^2 (1 - 4\tau \pm 2\lambda) = M^2 \left(1 - 4\tau \pm \frac{4\tau}{x} \right), \quad (5.1.36)$$

and the resulting Mandelstam plane is shown in Fig. 5.7. For real or virtual photons we have $\tau \geq 0$, and the physical region for $s \geq M^2$ corresponds to $0 \leq x \leq 1$. The Compton amplitude has non-analyticities arising from intermediate baryon resonances and baryon-meson continua. Hence, a theoretical handle on nucleon Compton scattering allows us to compute the nucleon's structure functions in DIS.

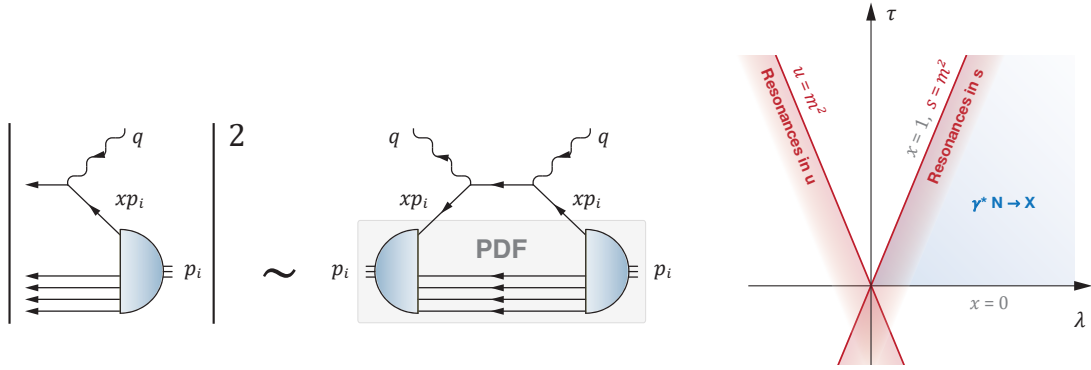


FIG. 5.7: Left: Hadronic tensor $W^{\mu\nu}$ in the parton model, and its relation with the forward Compton scattering amplitude and its factorized handbag structure. Right: Mandelstam plane in forward Compton scattering.

What about the PDFs? To begin with, it is important to realize that in the Bjorken limit the Fourier transform in Eq. (5.1.5) is dominated by the behavior close to the light cone $z^2 \rightarrow 0$, i.e., where the two interaction points are separated by a lightlike distance. This is easiest seen using **light-cone variables**:

$$a_{\pm} := \frac{1}{\sqrt{2}}(a^0 \pm a^3), \quad \mathbf{a}_{\perp} = (a^1, a^2) \quad \Rightarrow \quad a \cdot b = a_+ b_- + a_- b_+ - \mathbf{a}_{\perp} \cdot \mathbf{b}_{\perp}. \quad (5.1.37)$$

Then the integral (5.1.5) becomes schematically:

$$W(p, q) = \int dz_- e^{iq_+ z_-} \int dz_+ e^{iq_- z_+} \int_{z_{\perp}^2 < 2z_+ z_-} d^2 z_{\perp} e^{-iq_{\perp} \cdot z_{\perp}} W(p, z). \quad (5.1.38)$$

The domain of the z_{\perp} integration is restricted since the current commutator vanishes outside the light cone ($z^2 = 2z_+ z_- - z_{\perp}^2 < 0$) due to causality. In light-cone variables, the Bjorken limit $\nu \rightarrow \infty$, $x = \text{const.}$ corresponds to $q_+ \rightarrow \infty$ and $q_- = \text{const.}$:

$$\sqrt{2} q_{\pm} = q_0 \pm q^3 \stackrel{(4.5.27)}{=} \nu \pm \sqrt{\nu^2 - q^2} = \nu \left(1 \pm \sqrt{1 + \frac{2Mx}{\nu}} \right) \approx \begin{cases} 2\nu + Mx + \dots \\ -Mx + \dots \end{cases}$$

For $q_+ \rightarrow \infty$ and $q_- = \text{const.}$, the integral (5.1.38) is determined by the behavior of the integrand for $z_- \rightarrow 0$ and z_+ finite; this is the area with the least oscillations according to the Riemann-Lebesgue lemma. The condition $z_{\perp}^2 < 2z_+ z_-$ then implies $z^2 \rightarrow 0^+$ but $z^{\mu} \neq 0$, which is the light cone.

To proceed, we need to work out the current commutator in Eq. (5.1.5). We derived equal-time current commutators earlier in Eq. (3.1.57) using the anticommutation relations for the quark fields. For free fields one can generalize that formula to unequal times $x_0 \neq y_0$ with the generalized anticommutation relations

$$\{\psi(x), \bar{\psi}(y)\} = S(x - y), \quad \{\psi(x), \psi(y)\} = \{\bar{\psi}(x), \bar{\psi}(y)\} = 0, \quad (5.1.39)$$

where $S(z) := (i\not{\partial} + m)\Delta(z)$, and $\Delta(z)$ is the **causal propagator** which vanishes outside the light cone, i.e., for spacelike distances $z^2 < 0$:

$$\Delta(z) := \int \frac{d^3p}{2E_p} \frac{e^{-ipz} - e^{ipz}}{(2\pi)^3} \Big|_{p^0=E_p} = \int \frac{d^4p}{(2\pi)^3} e^{-ipz} \varepsilon(p^0) \delta(p^2 - m^2), \quad (5.1.40)$$

and $\varepsilon(a) = a/|a| = \Theta(a) - \Theta(-a)$ is the sign function. At equal times $z_0 = 0$, the causal propagators reduce to $\Delta(z) = 0$, $\partial_0\Delta(z) = -i\delta^3(\mathbf{z})$ and $S(z) = \gamma_0\delta^3(\mathbf{z})$ which reproduces the equal-time (anti-)commutation relations for scalar and fermion fields. (In contrast to the Feynman propagator (2.2.14), the causal propagator sums up the positive- and negative-energy pole residues of a free scalar propagator.)

Rederiving the current commutator relation in this case gives the result¹

$$\left[j_a^\Gamma(x), j_b^{\Gamma'}(y) \right] = if_{abc} j_c^+(x, y) + d_{abc} j_c^-(x, y) + \frac{\delta_{ab}}{N} j^-(x, y), \quad (5.1.41)$$

which depends on the bilocal currents

$$j_a^\pm(x, y) := \frac{1}{2} \left(\bar{\psi}(x) \Gamma S(x-y) \Gamma' \mathbf{t}_a \psi(y) \pm \bar{\psi}(y) \Gamma' S(y-x) \Gamma \mathbf{t}_a \psi(x) \right). \quad (5.1.42)$$

Here we recognize the ‘**handbag**’ structure from Fig. 5.7 when putting the result back in the hadronic tensor $W^{\mu\nu}$; for the electromagnetic current commutator we have $\Gamma = \gamma^\mu$ and $\Gamma' = \gamma^\nu$. The light-cone singularities come from the free propagator $S(z)$ which for a massless fermion reduces to

$$S(z) \xrightarrow{m=0} \frac{1}{2\pi} \not{\partial} (\varepsilon(z_0) \delta(z^2)). \quad (5.1.43)$$

It represents the hard part of the process, namely the scattering of the photon on a single perturbative quark which was the underlying assumption of the parton model.

The soft part is expressed through the remaining matrix element of bilocal quark-antiquark currents which is closely related to the quantity in Eq. (4.5.48). One can work out the Dirac structures for $\Gamma S(z)\Gamma'$ and $\Gamma' S(-z)\Gamma$ and expand the resulting currents in Taylor series about $z = 0$. This leads to the **operator product expansion (OPE)**, schematically written as

$$j\left(\frac{z}{2}, -\frac{z}{2}\right) = \sum_i c_i(z) \mathcal{O}_i(0), \quad (5.1.44)$$

where the $\mathcal{O}_i(0)$ are local operators and the $c_i(z)$ are the **Wilson coefficients**. The operators which are most important at high Q^2 are those for which the $c_i(z)$ are most singular as $z^2 \rightarrow 0$. This allows for a rigorous definition of PDFs that enter in Eq. (5.1.33) and makes them accessible for nonperturbative calculations.

Finally, the relation with the Compton amplitude also allows one to define non-forward **generalized parton distributions (GPDs)**. They encode the transverse structure of the proton, which is related to the orbital momentum carried by the quarks and gluons. In contrast to PDFs, they are no longer connected with DIS because a nonvanishing momentum transfer implies $p_f \neq p_i$. Hence, they have to be extracted directly from deeply virtual Compton scattering (DVCS) or related processes.

¹Extra care should be taken with regard to Schwinger terms, which include derivatives of the δ -function and do not show up in commutators of zero components of currents.